

Thermal emission from three-dimensional arrays of gold nanoparticles

Vassilios Yannopoulos*

Department of Materials Science, School of Natural Sciences, University of Patras, GR-26504 Patras, Greece

(Received 8 September 2005; revised manuscript received 6 January 2006; published 16 March 2006)

We study the blackbody spectrum from slabs of three-dimensional metalodielectric photonic crystals consisting of gold nanoparticles using an *ab initio* multiple-scattering method. The spectra are calculated for different photonic-crystal slab thicknesses, particle radii, and hosting materials. We find in particular that such crystals exhibit a broadband emission spectrum above a specific cutoff frequency with emissivity of about 90%. The studied photonic crystals can be used as efficient selective emitters and can therefore find application in thermophotovoltaics and sensing.

DOI: [10.1103/PhysRevB.73.113108](https://doi.org/10.1103/PhysRevB.73.113108)

PACS number(s): 42.70.Qs, 42.25.Dd, 71.23.An

The main feature of photonic crystals is the ability to tailor the photon density of states and this way control the spontaneous emission of light, aiming at the realization of new optoelectronic devices. In this context, there has been considerable effort to design and fabricate photonic crystals which allow for control of thermal emission of light, i.e., thermally driven spontaneous emission, promising applications in imaging, sensing, and most importantly, in thermophotovoltaics (TPV).^{1,2,4,3,5-9} Control of thermal emission can also be achieved by means of microstructured engineering on silicon¹⁰⁻¹³ or metal surfaces.¹⁴ Depending on the type of application, photonic crystals and structured surfaces can act as narrow- or wide-band, directional or isotropic thermal emitters. For example, in TPV applications¹⁵ a quasimonochromatic emission is preferable while in radiation cooling¹⁶ a broad emission spectrum is desired. In this work we investigate the emission properties of three-dimensional metalodielectric photonic crystals consisting of gold nanoparticles. We find, in particular, that the emission spectrum of these crystals can be such that photons are emitted in all directions only when their energies lie above a specific cutoff frequency, with emissivity as large as 90%.

Photonic crystals of spherical scatterers have been theoretically studied using multiple scattering theory^{17,18} which is ideally suited for the calculation of the transmission, reflection, and absorption coefficients of an electromagnetic (EM) wave incident on a composite slab consisting of a number of planes of nonoverlapping particles with the same two-dimensional (2D) periodicity. For each plane of particles, the method calculates the full multipole expansion of the total multiply scattered wave field and deduces the corresponding transmission and reflection matrices in the plane-wave basis. The transmission and reflection matrices of the composite slab are evaluated from those of the constituent layers. Having calculated these matrices one can evaluate the transmittance $\mathcal{T}(\omega, \theta, \phi)$, reflectance $\mathcal{R}(\omega, \theta, \phi)$, and from those two, the absorbance $\mathcal{A}(\omega, \theta, \phi)$ of the composite slab as functions of the incident photon energy $\hbar\omega$ and incident angles θ and ϕ . Transmittance and reflectance are defined as the ratio of the transmitted, respectively, the reflected, energy flux to the energy flux associated with the incident wave. The method applies equally well to nonabsorbing systems and to absorbing ones. In terms of speed, convergence and accuracy, the

multiple scattering method is the best method to treat photonic structures of spherical particles. The emittance $\mathcal{E}(\omega, \theta, \phi)$ is calculated indirectly by application of Kirchoff's law,^{19,20} i.e., from

$$\mathcal{E}(\omega, \theta, \phi) = \mathcal{A}(\omega, \theta, \phi) = 1 - \mathcal{R}(\omega, \theta, \phi) - \mathcal{T}(\omega, \theta, \phi). \quad (1)$$

Note that recent direct calculations of the thermal emission from photonic crystals have verified the validity of Kirchoff's law for the case of photonic crystals.²¹

In this work we deal with gold spheres with a radius of a few nanometres. Traditionally, the gold spheres are treated as plasma spheres whose dielectric function is given by Drude's formula

$$\epsilon_p(\omega) = 1 - \frac{\omega_p^2}{\omega(\omega + i\tau^{-1})}, \quad (2)$$

where ω_p stands for the bulk plasma frequency of the metal and τ is the relaxation time of the conduction-band electrons. The dielectric function $\epsilon(\omega) = \epsilon_1(\omega) + i\epsilon_2(\omega)$ for bulk gold has been determined experimentally by Johnson and Christy²² over the range from $\hbar\omega = 0.64$ eV to $\hbar\omega = 6.60$ eV. Taking $\hbar\tau^{-1} = \hbar\tau_b^{-1} = 0.027$ eV and $\hbar\omega_p = 8.99$ eV,^{25,26} Eq. (2) reproduces satisfactorily the experimentally determined $\epsilon_1(\omega)$ over the whole of the above frequency range, and the experimentally determined $\epsilon_2(\omega)$ at low frequencies. τ_b refers to the collision time of conduction-band electrons in the bulk metal; due to the finiteness of a nanosphere, the collision time τ of an electron in a sphere of radius S is decreased due to scattering at the boundaries of the sphere. It is given by

$$\tau^{-1} = \tau_b^{-1} + v_F S^{-1} \quad (3)$$

where v_F stands for the average velocity of an electron at the Fermi surface. For gold $\hbar v_F = 0.903$ eV nm,^{23,24} so that for a sphere of radius $S = 5$ nm, using $\hbar\tau_b^{-1} = 0.027$ eV, we obtain $\hbar\tau^{-1} = 0.21$ eV. Therefore, a more realistic description of the dielectric function of a gold sphere would be^{23,24}

$$\epsilon_s(\omega) = \epsilon(\omega) + \frac{\omega_p^2}{\omega(\omega + i\tau_b^{-1})} - \frac{\omega_p^2}{\omega(\omega + i\tau^{-1})}, \quad (4)$$

where $\epsilon(\omega)$ is the experimentally determined dielectric function of bulk gold. We note that $\epsilon_s(\omega)$ as given above, is

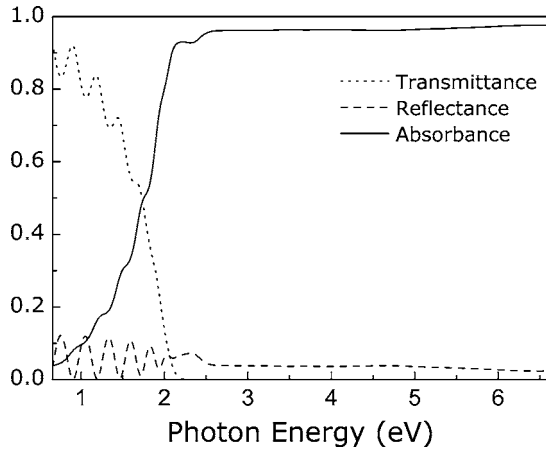


FIG. 1. Transmittance, reflectance, and absorbance of light incident normally on a 128-layers thick slab of a fcc crystal consisting of gold spheres ($S=5$ nm) in air ($\epsilon_h=1$), with $f=0.3$.

different from the approximation to the dielectric function of the gold sphere obtained from Eq. (2) with $\hbar\omega_p=8.99$ eV and $\hbar\tau^{-1}=0.21$ eV only because the imaginary part of the dielectric function is not represented well by Eq. (2) for $\hbar\omega > 1.5$ eV. Taking into account the finite size of a metal nanoparticle for the determination of the actual dielectric function, i.e., Eq. (4), has successfully reproduced experimentally obtained light absorption and scattering spectra of monolayers of gold nanoparticles.²⁷

To begin with, we consider a fcc photonic crystal whose lattice sites are occupied by gold nanospheres of radius $S=5$ nm. The lattice constant of the crystal is $a=19.11$ nm corresponding to a volume filling fraction occupied by the spheres, $f=0.3$. The spheres are supposed to be suspended in air. The crystal is viewed as a succession of planes of spheres (layers) parallel to the (001) surface of fcc. In Fig. 1 we show the transmittance, reflectance, and absorbance versus energy for light incident normally on a finite slab of the crystal consisting of 128 layers of spheres. We observe that for energies above 2.2 eV almost all light (92–98 %) that is incident on the crystal slab is absorbed from the gold spheres. Therefore, from Kirchoff's law, i.e., $\mathcal{E}(\omega, \theta, \phi) = \mathcal{A}(\omega, \theta, \phi)$, we can infer that the blackbody radiation is strong above this energy. Indeed, the blackbody radiation intensity of the photonic crystal is given by

$$I_{PC}(\omega, \theta, \phi, T) = \mathcal{E}(\omega, \theta, \phi) I_{BB}(\omega, T), \quad (5)$$

where $I_{BB}(\omega, \theta, \phi, T)$ is the blackbody radiation intensity (Planck distribution)

$$I_{BB}(\omega, T) = \frac{\hbar\omega^3}{4\pi^3 c^2} \frac{1}{\exp(\hbar\omega/k_B T) - 1}. \quad (6)$$

k_B is the Boltzmann constant and c is the speed of light in vacuum. In a metal particle of nanoscale radius, there are two principal sources of light emission/absorption: The first one is the dipole oscillations due to the surface plasmon resonances and the second is the interband transitions that take place in bulk gold contributing to its dielectric function. In terms of the first source of emission, the crystal can be

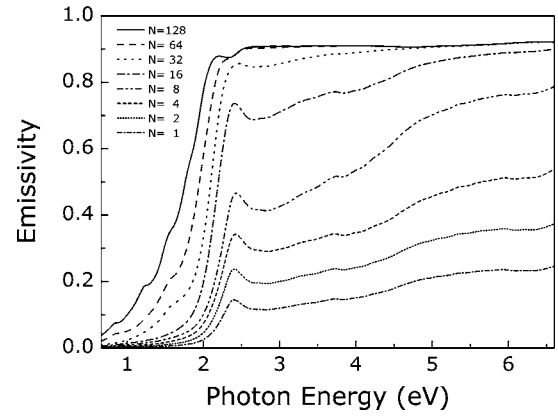


FIG. 2. SH emissivity for different numbers of layers (slab thicknesses) of the photonic crystal described in Fig. 1.

viewed as a lattice of interacting oscillating dipoles where each one of the dipoles emits light around the surface plasmon resonance frequency $\omega_{SP} = \omega_p / \sqrt{3}$. The interaction between the dipoles leads to the creation of a band of resonances around ω_{SP} . In two-dimensional systems, this band of resonances is manifested as a strong absorption/emission peak²⁸ while in three-dimensional systems, it is manifested as two absorption/emission peaks (corresponding to two bands of resonances) with a reflectivity peak (stemming from a photonic band gap) lying between them.²⁹ In Fig. 1 we cannot clearly identify surface plasmon peaks as these must have been submerged into the absorption edge due to interband transitions. In any case, both contributions (plasmon + interband) lead to a strong absorption/emission plateau above 2.2 eV.

As the system considered here can potentially find application in TPV devices we are interested in the spectral hemispherical (SH) radiative properties of the photonic crystal. More specifically, we are interested in the SH emissivity $s(\omega)$ which is the ratio of the SH emissive power of a photonic-crystal slab to the SH emissive power of a perfect blackbody at the same temperature T . For a slab infinitely extended in two dimensions

$$\begin{aligned} s(\omega) &= \frac{\int_0^{2\pi} d\phi \int_0^{\pi/2} d\theta I_{PC}(\omega, \theta, \phi, T) \cos \theta \sin \theta}{\int_0^{2\pi} d\phi \int_0^{\pi/2} d\theta I_{BB}(\omega, T) \cos \theta \sin \theta} \\ &= \frac{1}{\pi} \int_0^{2\pi} d\phi \int_0^{\pi/2} d\theta \epsilon(\omega, \theta, \phi) \cos \theta \sin \theta. \end{aligned} \quad (7)$$

Note that $\epsilon(\omega, \theta, \phi)$ in the above equation is the arithmetical average of both polarization modes. In Fig. 2 we show the SH emissivity from slabs of the photonic crystal of Fig. 1 for different slab thicknesses (number of layers). It is evident that as the number of layers increases the SH emissivity increases accordingly until it reaches a saturation plateau for slabs of 64 layers and above. Indeed, for energies above 2.2 eV the emissivity curves for 64 and 128 layers are practically the same. This fact implies that, if we measure the

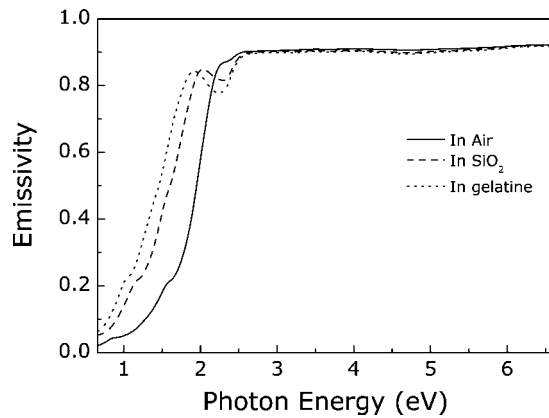


FIG. 3. SH emissivity of a 64-layer thick slab of an fcc crystal of gold spheres ($S=5$ nm) in air ($\epsilon_h=1$ —solid line), silica ($\epsilon_h=1.88$ —dashed line), and gelatine ($\epsilon_h=2.37$ —dotted line), with $f=0.3$. We have assumed that the host medium surrounding the spheres also covers the whole space.

emission from one of the surfaces of a 128 layers-thick slab, then the emitted radiation must be coming from the 64 outermost layers (relative to a given surface) while radiation coming from the 64 innermost layers is almost totally absorbed from the 64 outermost layers by the time it reaches the surface of the slab. The most important finding of Fig. 2 is the fact that the photonic crystal behaves more or less as gray body (emissivity ranging from 88 to 92 %) for energies above 2.2 eV while, at the same time, emits small amounts of radiation for energies below this cutoff. A similar emission spectrum is observed for the Salisbury screen¹³ but with significantly lower values of the SH emissivity.

So far, we have assumed that the gold nanospheres are suspended in air. In order to provide a manufacturable structure it is necessary to examine the case where the spheres are embedded in a host material of dielectric function ϵ_h . In Fig. 3 we show the SH emissivity from a 64-layer slab of an fcc photonic crystal of gold nanospheres with $f=0.3$ where the spheres are surrounded by air ($\epsilon_h=1$), silica ($\epsilon_h=1.88$), and gelatine ($\epsilon_h=2.37$). The introduction of a host material does not change the picture drastically except that it lowers the emission cutoff energy. This is due to the lowering of the surface plasmon frequency according to $\omega_{SP}=\omega_p/\sqrt{1+2\epsilon_h}$ when a nanosphere is placed in a host medium ϵ_h , which results in strong thermal emission at lower energies. As a result of the energy shift of the surface plasmon resonance, the corresponding emission peak moves away from the interband emission region and a distinct local minimum appears. This is evident from the emissivity spectra of Fig. 3 for silica and gelatine host materials. The shift of the surface plasmon energy with respect to the host material ϵ_h allows for tuning of the cutoff energy so that it coincides with the band gap of the photodiode of a TPV device.

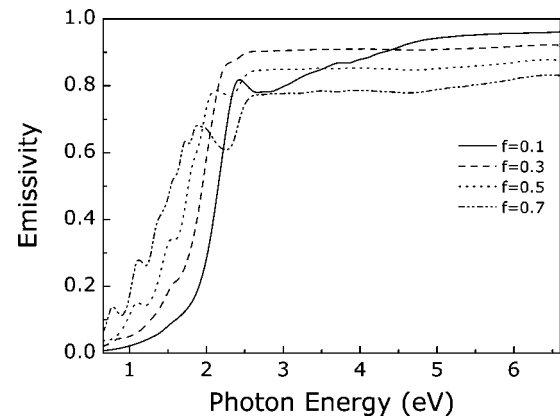


FIG. 4. SH emissivity of a 64-layer thick slab of an fcc crystal of gold spheres ($S=5$ nm) in air, for different volume filling fractions f (fixed lattice constant and different sphere radii).

Next we study the effect of the volume filling fraction f on the emission properties of the photonic structure under study. In Fig. 4 we show the SH emissivity spectra for photonic crystals of different values of f . We have kept the lattice constant the same and changed the sphere radii accordingly. Note that for each value of f we obtain a different value of $\hbar\tau^{-1}$ from Eq. (3). We observe that the maximum emissivity in the region above the cutoff energy is achieved for $f=0.3$. Since our calculations show that the SH reflectivity assumes higher values for $f=0.5, 0.7$, the radiation emitted from the innermost layers is reflected back and reabsorbed before it reaches the surface of the slab.

Finally we address the issue of spatial order/disorder of the photonic crystal under investigation. As it has been both theoretically^{30,31} and experimentally³² shown, the presence of disorder does not change practically the absorption/emission properties of three-dimensional photonic crystals of metal nanoparticles since these quantities mostly depend on single sphere properties such as surface plasmon resonances, and less on the particular spatial arrangement of the spheres. Note that this is not true for one- or two-dimensional structures, e.g., a linear chain or a monolayer of nanospheres, where the presence of disorder changes dramatically the absorption/emission spectra.³¹ So, since we deal with a three-dimensional structure, a disordered crystal might be easier and cheaper to fabricate.

In summary, we have shown that a metallodielectric crystal consisting of gold nanospheres can act as a 90% gray body for energies above a cutoff. The cutoff frequency can be tuned by an appropriate choice of the material hosting the nanospheres. Optimal emissivity is obtained for moderate volume filling fractions and slab thicknesses.

This work was supported by the “Karatheodory” research fund of the University of Patras.

*Electronic address: vyannop@upatras.gr

- ¹C. M. Cornelius and J. P. Dowling, Phys. Rev. A **59**, 4736 (1999).
- ²S. Y. Lin, J. G. Fleming, E. Chow, J. Bur, K. K. Choi, and A. Goldberg, Phys. Rev. B **62**, R2243 (2000).
- ³J. G. Fleming, S. Y. Lin, I. El-Kady, R. Biswas, and K. M. Ho, Nature (London) **417**, 52 (2002).
- ⁴M. U. Pralle, N. Moelders, M. P. McNeal, I. Puscasu, A. C. Greenwald, J. T. Daly, E. A. Johnson, T. George, D. S. Choi, I. El-Kady, and R. Biswas, Appl. Phys. Lett. **81**, 4685 (2002).
- ⁵S. Y. Lin, J. G. Fleming, and I. El-Kady, Opt. Lett. **28**, 1909 (2003).
- ⁶I. Celanovic, F. O' Sullivan, M. Ilak, J. Kassakian, and D. Perreault, Opt. Lett. **29**, 863 (2004).
- ⁷A. Narayanaswamy and G. Chen, Phys. Rev. B **70**, 125101 (2004).
- ⁸S. Enoch, J.-J. Simon, L. Escoubas, Z. Elalmy, F. Lemarquis, P. Torchio, and G. Albrand, Appl. Phys. Lett. **86**, 261101 (2005).
- ⁹M. Florescu, H. Lee, A. J. Stimpson, and J. Dowling, Phys. Rev. A **72**, 033821 (2005).
- ¹⁰H. Sai, H. Yugami, Y. Akiyama, Y. Kanamori, and K. Hane, J. Opt. Soc. Am. A **18**, 1471 (2001).
- ¹¹S. Maruyama, T. Kashiwa, H. Yugami, and M. Esashi, Appl. Phys. Lett. **79**, 1393 (2001).
- ¹²F. Marquier, K. Joulain, J. P. Mulet, R. Carminati, and J. J. Greffet, Opt. Commun. **237**, 379 (2004).
- ¹³M. Laroche, F. Marquier, R. Carminati, and J. J. Greffet, Opt. Commun. **250**, 316 (2005).
- ¹⁴F. Kusunoki, T. Kohama, T. Hiroshima, S. Fukumoto, J. Takahara, and T. Kobayashi, Jpn. J. Appl. Phys., Part 1 **43**, 5253 (2004).
- ¹⁵M. Zenker, A. Heinzl, G. Stollwerck, J. Ferber, and J. Luther, IEEE Trans. Electron Devices **48**, 367 (2001).
- ¹⁶C. W. Hoyt, M. P. Hasselbeck, M. Sheik-Bahae, R. I. Epstein, S. Greenfield, J. Thiede, J. Distel, and J. Valencia, J. Opt. Soc. Am. B **20**, 1066 (2003).
- ¹⁷N. Stefanou, V. Karathanos, and A. Modinos, J. Phys.: Condens. Matter **4**, 7389 (1992).
- ¹⁸N. Stefanou, V. Yannopapas, and A. Modinos, Comput. Phys. Commun. **113**, 49 (1998); **132**, 189 (2000).
- ¹⁹S. M. Rytov, Yu. A. Kravtsov, V. I. Tatarskii, *Principles of Statistical Radiophysics, Elements of Random Fields* Vol. 3 (Springer, Berlin, 1989).
- ²⁰J. J. Greffet and M. Nieto-Vesperinas, J. Opt. Soc. Am. A **15**, 2735 (1998).
- ²¹C. Luo, A. Narayanaswamy, G. Chen, and J. D. Joannopoulos, Phys. Rev. Lett. **93**, 213905 (2004).
- ²²R. B. Johnson and R. W. Christy, Phys. Rev. B **6**, 4370 (1972).
- ²³S. Norrman, T. Andersson, C. G. Granqvist, and O. Hunderi, Phys. Rev. B **18**, 674 (1978).
- ²⁴F. Abelès, Y. Borensztein, and T. López-Rios, *Festkörperprobleme (Advances in Solid State Physics)* (Braunschweig, Vieweg, 1984), Vol. 24, p. 93.
- ²⁵M. M. Wind, P. A. Bobbert, J. Vlieger, and D. Bedeaux, Physica A **143**, 164 (1987).
- ²⁶P. A. Bobbert and J. Vlieger, Physica A **147**, 115 (1987).
- ²⁷N. Stefanou and A. Modinos, J. Phys.: Condens. Matter **3**, 8135 (1991).
- ²⁸N. Stefanou and A. Modinos, J. Phys.: Condens. Matter **3**, 8149 (1991).
- ²⁹V. Yannopapas, A. Modinos, and N. Stefanou, Phys. Rev. B **60**, 5359 (1999).
- ³⁰A. Modinos, V. Yannopapas, and N. Stefanou, Phys. Rev. B **61**, 8099 (2000).
- ³¹V. Yannopapas, A. Modinos, and N. Stefanou, Opt. Quantum Electron. **34**, 227 (2002).
- ³²K. P. Velikov, W. L. Vos, A. Moroz, and A. van Blaaderen, Phys. Rev. B **69**, 075108 (2004).